Synthesis And Characterization of Terbium (Tb) And Europium (Eu) Doped Mixed Ferrites

Nawal Kishore[1] and S. Mukherjee[2]
[1]Dept. of Electronics and Communications, University College of Engineering and Technology.
Vinoba Bhave University, Hazaribag-825301, Jharkhand, India
[2]Dept. of Applied Physics, Birla Institute of Technology, Mesra, Ranchi - 835215, Jharkhand, India

Abstract **- $Eu_xNi_{1-x}Fe_2O_4$, and $Tb_xNi_{1-x}Fe_2O_4$ where "x" varies as 0.02, 0.05, 0.1 two sets of series of samples have been prepared. The samples have been prepared by chemical co-precipitation route. For the first series, calculated amount of salt of Eu, Fe and Ni were dissolved in de -ionized water and stirred for a few minutes. 0.1 M (Molar) NH_4OH solution was then slowly added drop wise under vigorous stirring. The alkali addition was continued till the pH of the solution was 10 and was left undisturbed for 1 hour for complete digestion. The precipitate was then washed thoroughly till pH 7 and then heated to 600^0C. Next set of series prepared with same synthesis steps. The samples were checked for their phase purity by x ray diffraction which confirmed the spinel phase.**
.

Keywords: **Nanocrystalline, spinel structure, chemical co precipitation, XRD (x-ray diffraction), Spectroscopy, JCPDS (joint committee for powder diffraction standards)**

1. INTRODUCTION

Iron oxide material that has lots of opportunity in research for its many possible applications, due primarily to its magnetic and electrical properties.

Ferrimagnetic materials based on ferrites have been contributing in various applications like radio frequency circuit, antennas application, information storage, targeted drug delivery, MRI (Magnetic Resonance Imaging) scanning, microwaves read/write heads for high speed digital tapes and other devices. Based on the crystal structure there are three types of ferrites [1-3].

Spinel: with cubic crystal structure and general formula $M^{2+}Fe_20_4$ where M = Fe, Ni, Mg, Zn, Co, or a mixture of these

Garnet: with cubic crystal structure and general formula $Ln_3^{3+}Fe_5O_{I2}$ where Ln = Y, Eu, lb, Ho, Lu.

Magnetoplumbite: with hexagonal crystal structure and general formula $M^{2+}Fe_{12}0_{19}$ where M = Ba or Sr.
Spinel ferrites are the simplest of these three groups having Close packed cubic structure of form AB_2O_4 Where, A= divalent cation, B= Trivalent cation. Cation has 4 or 6 co-ordination and form tetrahedral (A) and octahedral (B) Sub lattices. Here we are interested in nanoparticles of ferrites, the challenges in preparation of nanoparticles are to control the nanoparticles size, shape and properties, to assemble the nanoparticles for a given purpose. Nano mixed ferrites belonging to the Series $Tb_xNi_{1-x}Fe_2O_4$, and $Eu_xNi_{1-x}Fe_2O_4$ (for x= 0.02, 0.05, 0.1) by low cost and simple method like chemical Co-precipitation technique and evaluating the impact of Terbium (Tb) and Europium (Eu) substitution on the structural properties through X-ray diffractometry and detailed analysis of the Electrical properties of the series $Tb_xNi_{1-x}Fe_2O_4$, and $Eu_xNi_{1-x}Fe_2O_4$
(For x=0.02, 0.05, 0.1) through Impedance spectroscopy. Distribution of cations in octahedral and tetrahedral lattice is studied through Raman spectroscopy

2. EXPERIMENTAL

The nanocrystalline mixed ferrite material of Terbium nickel ferrite $Tb_xNi_{1-x}Fe_2O_4$, and Europium nickel ferrite $Eu_xNi_{1-x}Fe_2O_4$ (for x= 0.02, 0.05, 0.1) prepared by chemical co-precipitation method For the first series, calculated amount of salts of Eu, Fe and Ni were dissolved in deionized water and stirred for a few minutes. 0.1 M (molar) NH_4OH solution was then slowly added drop wise under vigorous stirring. The alkali addition was continued till the pH value of the solution was 10 and was left undisturbed for 1 hour for complete digestion. After chemical co-precipitation nanoparticles formed in the bottom of beaker from supernatant by centrifuge machine operating at a speed of 2200 rpm and duration is fixed at 4 or 5 minutes, the centrifugal process is continued till the pH reached at 7 after this we done the centrifugal process with alcohol we repeat this process at least 2 times with alcohol and then obtained the final product but it is still in wet condition so left it for whole day to dried it. By repeating whole process we prepare two series of samples in first series where 'x' varies 0.02, 0.05 and 0.1 is heat treated at 600 ^{0}C for 8 hours and again 500 ^{0}C for 8 hours same applied for second series also. After calculation we have required weight of Fe, Ni, Tb, and Eu in 250ml for 0.04M is 0.7985gm, 0.7469gm, 2.5832gm respectively.

3. RESULTS AND DISCUSSION

3.1 X-RAY DIFFRACTION:

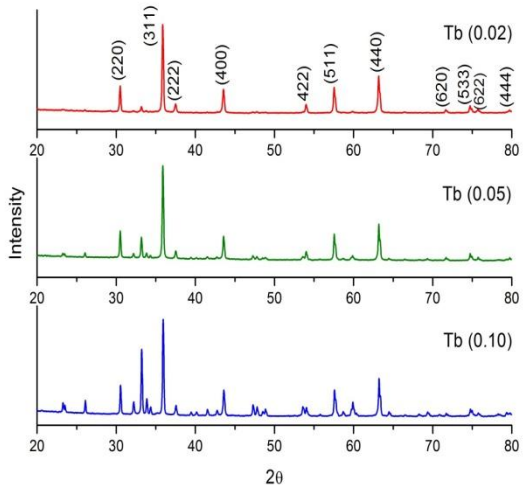

Fig 3.1.1 XRD pattern of $Tb_xNi_{1-x}Fe_2O_4$, (Terbium Nickel Ferrite) where "x" varies as 0.02, 0.05, 0.1

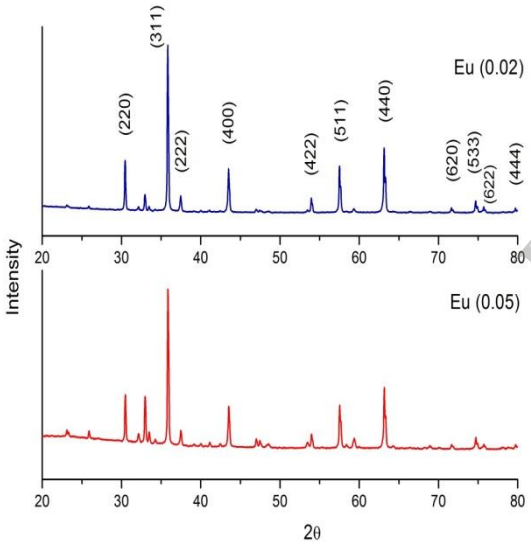

Fig 3.1.2 XRD pattern of $Eu_xNi_{1-x}Fe_2O_4$ (Europium Nickel Ferrite) where "x" varies as 0.02, 0.05, 0.1

XRD pattern of samples with generic formulas are: $Tb_xNi_{1x}Fe_2O_4$ (Terbium Nickel Ferrite), $Eu_xNi_{1x}Fe_2O_4$ (Europium Nickel Ferrite), where 'x' varies 0.02, 0.05 and 0.1 for Terbium nickel ferrite and 0.0, 0.05 for Europium doped ferrite sample the peaks in XRD patterns illustrate the characteristic peaks of single phase cubic spinel structure. Peak intensity is indicative of high degree of crystallinity of prepared ferrites. The existence of the (220), (311), (222), (400), (422), (511), (440), (620), (533), (622), and (444) major lattice planes in the XRD patterns confirms the formation of spinel cubic structure with the Fd3m space group, which is consistent with the powder diffraction file of JCPDS. The patterns were compared with standard data (JCPDS PDF card No. 089-4927), the mean particle sizes (D) were calculated from the X-ray line broadening of the (311) diffraction peak using the Scherrer's equation

$$D = k \lambda / \beta \cos\theta \qquad (1)$$

Where D is the crystallite size, λ is the wavelength of X-ray radiation, θ is the Bragg angle and β is the full width at half maximum (FWHM). From the analysis of the XRD spectra we found that the mean particle diameter (D) is nearly the same for all synthesized specimens, ranging from 43- 48 nm which shown in table 1 and table 2

Sample Name	2θ	FWHM (β) in radians	Average size of the particle (Nm approx.)
$Tb_{0.02}Ni_{0.98}Fe_2O_4$	35.89	0.19	43
$Tb_{0.05}Ni_{0.95}Fe_2O_4$	35.91	0.18	44
$Tb_{0.1}Ni_{0.9}Fe_2O_4$	35.94	0.17	47

Table 1 – Average particle size estimated from the diffraction spectrum in Figure 3.1

Sample Name	2θ	FWHM (β) in radians	Average size of the particle (Nm approx.)
$Eu_{0.02}Ni_{0.98}Fe_2O_4$	35.86	0.17	48
$Eu_{0.05}Ni_{0.95}Fe_2O_4$	35.88	0.18	47

Table 2 – Average particle size estimated from the diffraction spectrum in Figure 3.2

3.2 Dielectric Studies:

The samples for dielectric measurement were prepared with the help of palletizer of 12mm dia and applying a pressure of 120-150 Kg/cm^2 tones to get compact circular pellets with dimensions 12mm in diameter and approximately O.5mm to 2mm in thickness.

The dielectric constant measurements of the samples at low and high frequencies from a few Hz to 10 MHz were carried out by a Alpha-A High Performance Modular Measurement System. The dimension of pallet was suited for the measuring instrument. The dielectric constant of the sample can be calculated using the equation,

$\varepsilon_r=(c\ d/\ \varepsilon_0\ A)$ (2)

Where,

A= area of sandwiched structure

c= Capacitance measured by LCR

d = Thickness,

ε_0 = Absolute permittivity

Koop's and Maxwell Wagner theory can satisfactorily explain the dielectric behavior of ferrites [5]

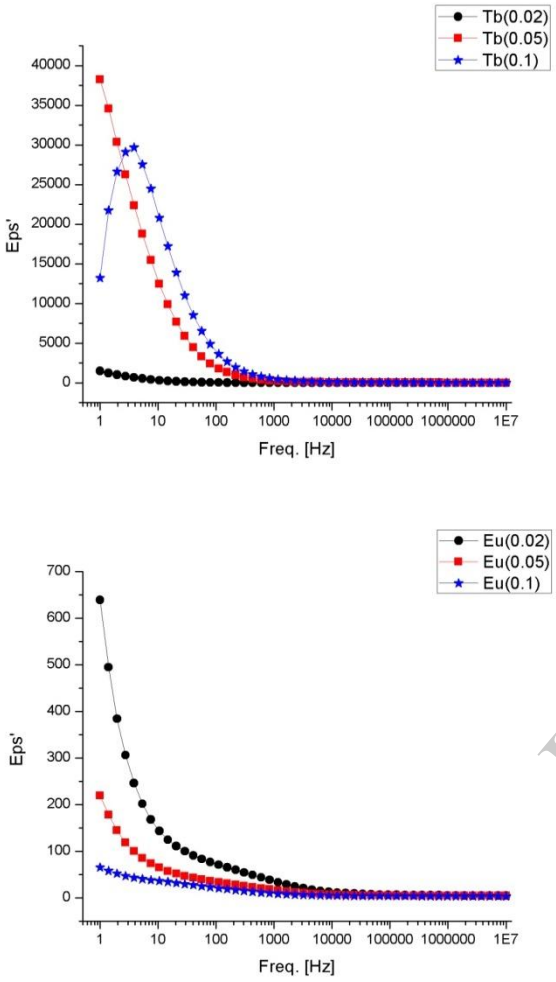

Fig 3.2.1 dielectric permittivity ε' vs. frequency with increasing doping of Tb, Eu

Fig 3.2.1 shows the relation of dielectric permittivity with the increasing frequency, the value decreases with increase in frequencies. with the increase of Tb/Eu concentration decrease in Ni^{+2} nickel ions as well as presence of Fe^{+2} ions in octahedral site also reduced, hence the number of Ni^{3+}/Ni^{2+} pair available for hole and electron hopping will be less in number which results less no. of pairs for hole and electron hopping, As hopping decreases now ion are started collected at the grain boundaries so the resistance of the grain boundaries increases and hence the possibility of charged species to cross over the grain boundaries decrease This will turn result in reduced hopping [4]

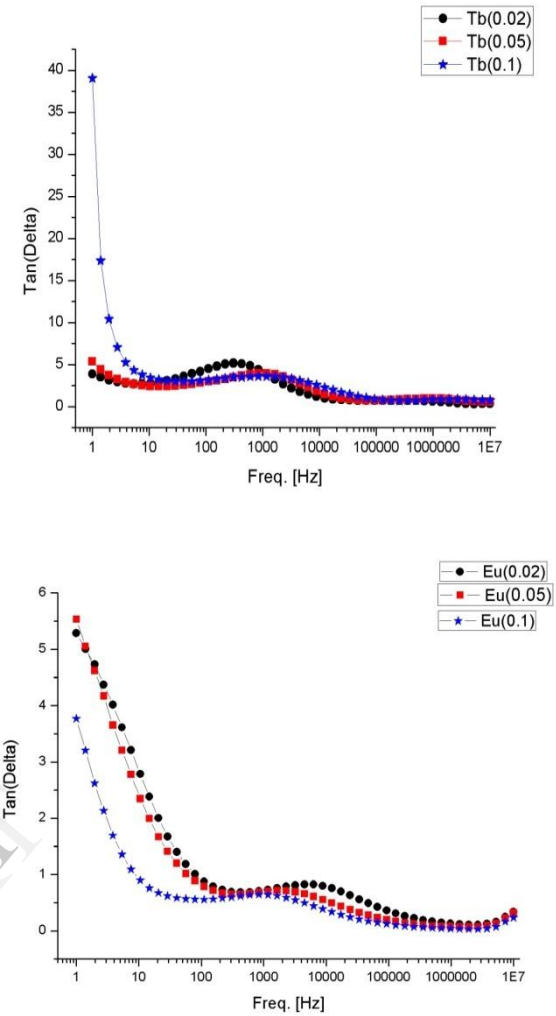

Fig 3.2.2 loss tangent (tan∂) vs. frequency with increasing doping of Tb, Eu

Fig 3.2.2 shows the loss tangent (tanδ) against frequency exhibit relaxation at specific frequencies Dielectric relaxation occur when the hopping frequency of charge carriers is equal to the frequency of the applied field [6], it is noticed that relaxation is absent or less in Eu/Tb rich components this may be due to the less number of availability of charge concentration for hopping,

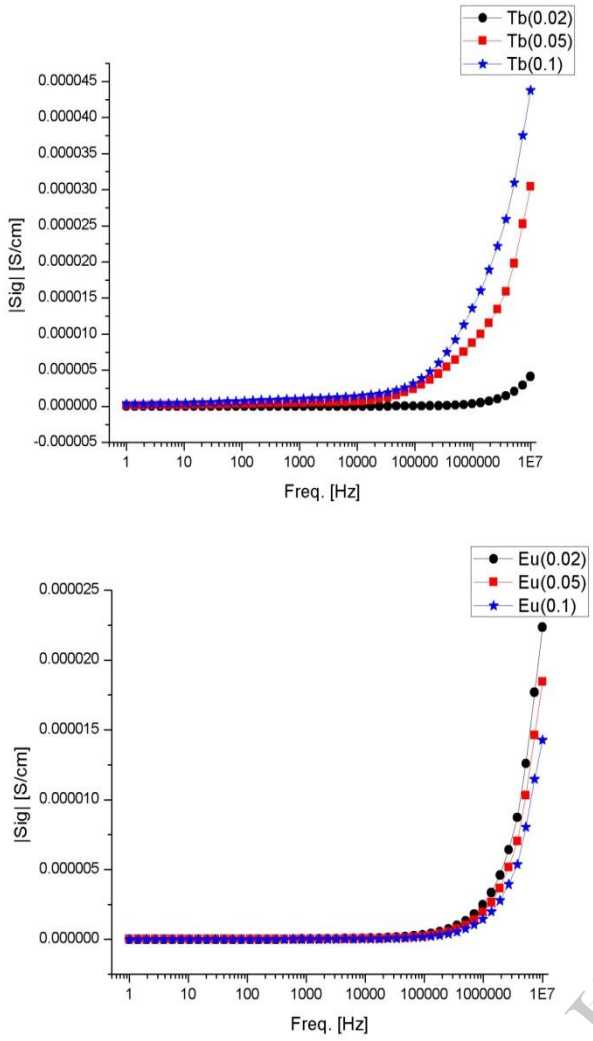

Fig 3.2.3 conductivity vs. frequency with increasing doping concentration of Tb, Eu**.**

In the case of Terbium Nickel ferrite and Europium Nickel ferrite electron hopping between Fe^{3+}/Fe^{2+}ions and hole hopping between Eu^{2+}/Eu^{3+} and Tb^{2+}/ Tb^{3+} ions are found to be responsible for electrical conduction[7].
Thus conductivity is found to depend on the availability of Fe^{2+}/Fe^{3+} ions and M^{2+}/M^{3+} where M=(Eu/Tb) pairs in octahedral sites. As the frequency of the applied field increases, hopping of charge carriers also increases thereby increasing the conductivity as shown in fig 3.2.3 .But as the frequencies increases the hopping of charge carriers could not follow the applied field frequency and it lags behind the applied frequency resulting in a decrease in the ac conductivity values.

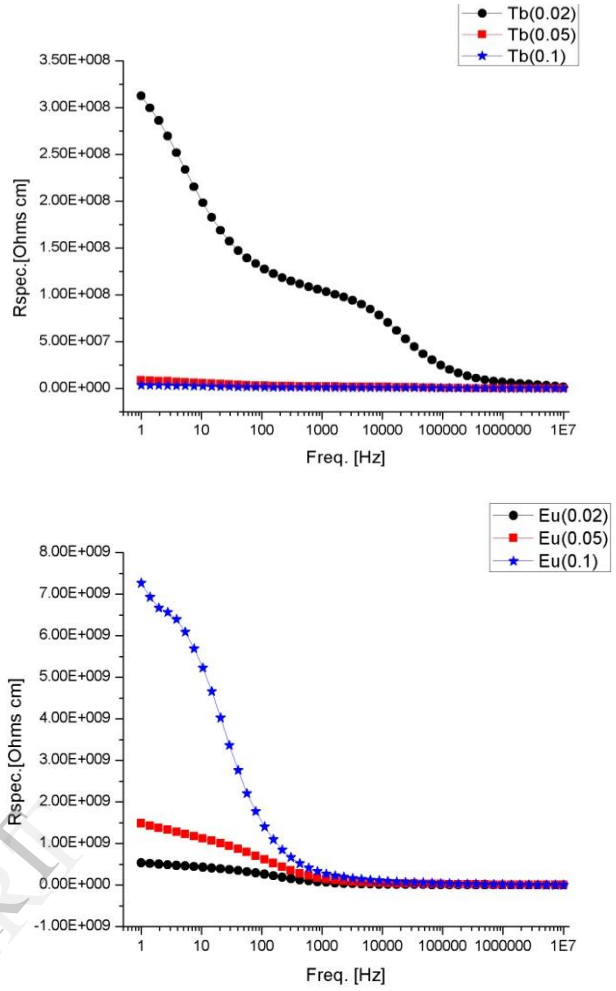

Fig 3.2.4 resistivity vs. frequency with increasing doping concentration of Tb, Eu.

The inverse of conductivity is resistivity and its graph shown in fig 3.2.4. With increasing doping content there is a decrease Fe^{2+} ions in the octahedral sites is also reduced .Hence the number of Ni^{2+}/Ni^{3}, Eu^{2+}/Eu^{3+}, $Tb^{2+}/ Tb^{3+}$and Fe^{3+}/Fe^{2+} pairs available for hole and electron hopping will be less in number as we increase the Terbium or Europium content as a result hopping decreases and the charged species are accumulated at the grain boundaries. Therefore the resistance of the grain boundaries increases and hence the resistivity increases the probability of charged species to cross over the grain boundaries decreases.

3.3 RAMAN SPECTROSCOPY:

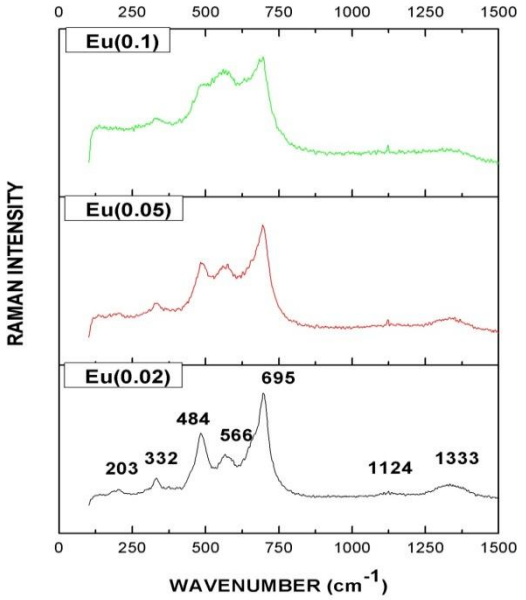

Fig 3.3.1 Raman spectroscopy of $Eu_xNi_{1-x}Fe_2O_4$(x=0.02, 0.05, 0.1)

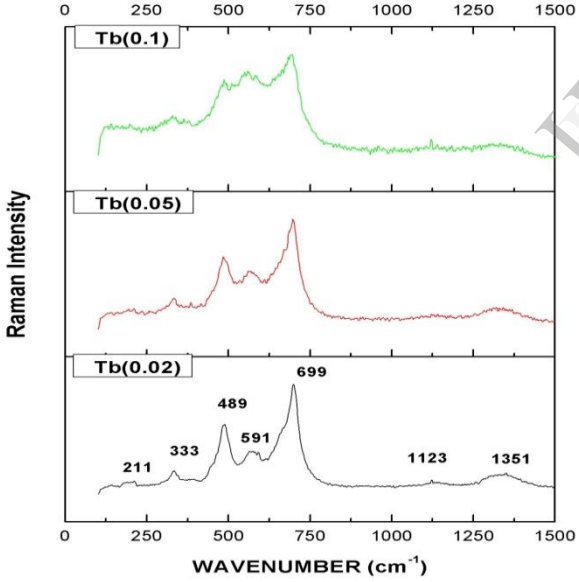

Fig 3.3.2 Raman spectroscopy of $Tb_xNi_{1-x}Fe_2O_4$(x=0.02, 0.05, 0.1)

Raman spectra of $Eu_xNi_{1-x}Fe_2O_4$ and $Tb_xNi_{1-x}Fe_2O_4$ sample where "x' varies from 0.0 to 0.5 observed in the range of 0 - 1500 cm^{-1}, the vibrational modes are around at 203cm^{-1}, 332cm^{-1}, 484cm^{-1}, 566cm^{-1}, 695cm^{-1}, 1124cm^{-1}, 1333cm^{-1} (for Europium doped samples) and 211cm^{-1}, 333cm^{-1}, 489cm^{-1}, 591cm^{-1}, 699cm^{-1}, 1123cm^{-1}, 1351cm^{-1} (for Terbium doped samples) respectively from the fig 3.3.1 and fig 3.3.2 The hyperfine associated to both crystallographic sites octahedral(A) and tetrahedral (B) Of samples $Eu_xNi_{1-x}Fe_2O_4$ and $Tb_xNi_{1-x}Fe_2O_4$ (x=0.02, 0.05, 0.1), 0.1)decreases as the Eu/Tb content increases, it can be easily observed in fig 3.3.1 and fig 3.3.2 and this can be explained considering the super exchange interaction among the neighboring metal ions in the spinel structure [8]. With increasing Eu/Tb content the probability of the Fe ions to find Eu/Tb ion as nearest neighboring increases, thus hyperfine decreases. Further, the Raman frequency depends on the Fe (Eu/Tb)-O bond length, which changes with both the variation of the lattice parameter and ionic radii of divalent ions. Intensity of the highest wavelength Raman mode initially around 695$cm^{-1}$for Eu and 699cm^{-1} for Tb decreases with increasing Eu/Tb content.

4. CONCLUSION

The synthesis process used is very simple and easily performed. Nanocrystalline europium and terbium doped Nickel ferrite for x= 0.02, 0.05, 0.1 were prepared using wet chemical co-precipitation technique. The prepared samples exhibiting a spinel structure with sizes varying from 43nm– 47nm. for europium and terbium doped Nickel ferrite, The XRD pattern obtained have some extra phase due to the impurities mixing during processing condition , but overall result of XRD pattern confirms the spinel cubic structure with high degree of crystallinity. The decrease in size and the contraction of lattices with increasing Tb/ Eu concentration in the nanoparticles. Sharpness of peaks indicated the highly crystalline nature of the precipitate. $Eu_xNi_{1-x}Fe_2O_4$ and $Tb_xNi_{1-x}Fe_2O_4$ (x=0.02, 0.05, 0.1) nanoparticles were studied. The low frequency dielectric dispersion was explained in terms of Maxwell-Wagner theory, the effect of grains and grain interfaces enhanced in the nanoregime the decrease in Permittivity (ε) with Tb/Eu substitution point to the decrease in availability of Ni^{2+}/Ni^{3+} and Fe^{2+}/Fe^{3+} pair. The loss tangent (tanƋ) exhibit strong relaxation. Relaxation peaks and relaxation time (Γ) was estimated from these relaxations. Raman spectra of $Eu_xNi_{1-x}Fe_2O_4$ and $Tb_xNi_{1-x}Fe_2O_4$ sample where "x'' varies from 0.0 to 0.5 observed in the range of 0 - 1500 cm^{-1}, the vibrational modes of Raman confirms the existence of five Raman modes and distribution of cation in octahedral and tetrahedral sub lattices in agreement with the as-synthesized samples.

5. REFERANCES

[1]. J. Smil, and H.PJ. Wijn, Ferrites, Philips Technical Library Netherlands (1959).
[2]. Charles Kittel, Introduction to Solid State Physics, 7111 Edition, John Wiley & Sons, Inc., Singapore (1996).
[3]. R. Valenzuela, Magnetic Ceramics, Cambridge University Press, (1994) London.
[4]. Veena Gopalan E. "On the Synthesis and Multifunctional Properties of some Nanocrystalline Spinel Ferrites and Magnetic Nanocomposites", Ph.D. Thesis (Department of Physics Cochin University), June 2009.
[5]. P. Chandra Mohan, M.P Srinivasan, S. Velmurugan and S.V Narasimhan Journal of Solid State chemistry 184, 89(2011).
[6]. A. M. Abo et al. and S M Attia, J. Magn. Mag. Mat, 257, 2003), 165.
[7]. A.M Abdeen, Journal of Magn.Mag.Mat, 192, (1999), 121.
[8]. C. M. Srivastava, S. N. Shringi, and R. G. Srivastava, Phys. Rev. B 14, 2041 (1976).